NTNU – Trondheim
Norwegian University of
Science and Technology

Characterization and recovery of rare earth elements from electronic scrap

Lene Marie Lysgaard Bristøl

Preface

This project work was conducted at Norwegian University of Science and Technology, NTNU, as a part of the Materials Chemistry and Energy Technology, Master Thesis, TMT4900, spring semester 2011.

First I want to thank my supervisor, Gabriella Tranell, for her guidance and the possibility to work within such an interesting field of research. Secondly I want to express my gratitude to my co-supervisor, Ragnhild E. Aune, for her help and valuable inputs.

Thank you to WEEE Recycling AS for the cooperation and the materials.

Finally I want to thank those who helped me with my experiment and the analysis; Delphine Leroy, Egil Krystad, Yingda Yu and Pei Na Kui at IMT, Torill Sørløkk and Erik Larsen at IGB.

The work described in this thesis has been done individually and in accordance with NTNU regulations.

Trondheim, 15.06.2012
Lene M. L. Bristøl

Abstract

The rare earth elements are a group of 17 elements consisting of the lantahnide series, scandium and yttrium. The application with the largest rare earth consumption is the permanent rare earth magnets. The neodymium-iron-boron magnets are the strongest permanent magnetic material known and are widely used. There is a concern that there will be a shortage in Nd-Fe-B magnets in short time. This has lead to an increased interest in the recycling of the rare earth magnets in the world.

This project gives a very brief introduction to the Nd-Fe-B magnets, their uses and recycling. Two types of experiments that aims at recovery of neodymium from Nd-Fe-B magnets have been performed; extraction of neodymium by the use of molten silver and extraction of neodymium by direct oxidation.

In the liquid silver experiments, extraction was obtained, but the analysis gave equivocal results.

In the direct oxidation experiment, the separation of an iron phase and a neodymium oxide phase failed, and the experiment was not seen as successful.

Magnetic waste from WEEE Recycling was also performed, and it turned out to contain small amounts of rare earth elements.

Sammendrag

De sjeldne jordmetallene er en gruppe av 17 grunnstoffer som består av lantanidene, scandium og yttrium. De sjeldne jordmetallene har mange anvendelser, men den anvendelsen som bruker mesteparten av gruppen er permanente magneter. Neodym-jern-bor magnetene er det sterkeste permanente magnetisk materialet som er kjent, og er mye brukt. Det er forventet en mangel av Nd-Fe-B magneter om kort tid, og dette har ført til en økt interesse for resirkulering av sjeldne jordmetallbaserte magneter i hele verden.

Dette prosjektet gir en kort introduksjon til Nd-Fe-B magneter, deres anvendelser og resirkulering. To typer eksperiment med formål å gjenvinne neodym fra Nd-Fe-B magneter har blitt utført; ekstraksjon av neodym ved bruk av smeltet sølv og ekstraksjon av neodym ved direkte oksidering.

I ekstraksjonseksperimentene med bruk av sølv ble ekstraksjon oppnådd, men analysen ga tvetydige resultater.

I eksperimentene med direkte oksidasjon feilet separasjonen av en jernfase og en neodymoksid-fase, og eksperimentene ble ikke betraktet som vellykket.

Magnetisk avfall fra WEEE Recycling AS ble karakterisert, og det viste seg å være små mengder sjeldne jordmetaller i avfallet.

Contents

List of Figures

1 Introduction

1.1 Background

The rare earth elements are a group of 17 elements consisting of the lanthanide series, scandium and yttrium (IUPAC, 2005). All elements occur naturally except promethium, Pm, which is exclusively radioactive and has no stable isotopes (Gupta & Krishnamurthy, 2005). The rare earth elements are highlighted in yellow in the periodic table in Figure 1.

Figure 1: The Rare Earth Elements (Bristøl, 2011)

The rare earth elements are produced from rare earth containing ores, mainly as byproducts in mining of other elements (Öko-Institut, 2011). The production can be done through many different processes, but metallothermic and electrolytic methods have been the most successful (Gupta & Krishnamurthy, 2005).

Rare Earth elements are used in many high technology applications like permanent magnets, batteries, phosphors and lasers. Figure 2 shows the rare earth consumption by weight for different applications (Oakdene Hollins, 2010). There are concerns that the demand of these elements will exceed the supply in few years (Oakdene Hollins, 2010).

China accounts for 97% of the world's rare earth production, and recent documentation indicates that China has decided to reduce the export of rare earth elements (Oakdene Hollins, 2010). It has been estimated that by 2015,
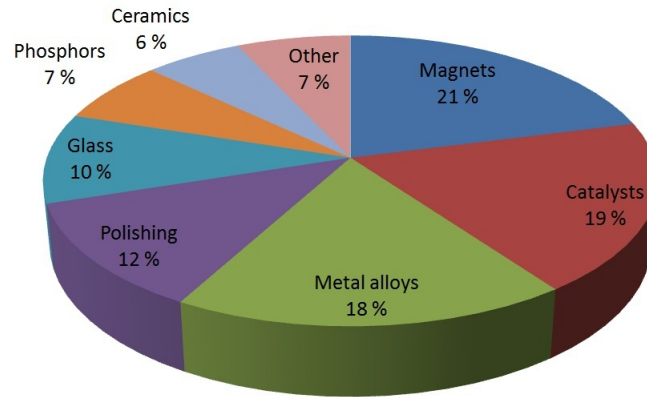
Figure 2: Applications of the Rare Earth Elements (Bristøl, 2011)

China will no longer export rare earth metals. This has lead to an increased interest in production and recycling of rare earth elements in the rest of the world.

The EU consider the rare earth metals to be highly critical materials, which means that they have a high economic importance to the EU combined with high supply risk (EPOW, 2011a).

The application with the highest consumption of rare earth elements is magnets (Oakdene Hollins, 2010). There are two types of rare earth magnets; the neodymium-iron-boron- and the samarium-cobalt magnets (EPOW, 2011a). They are the strongest permanent magnetic materials known, and the neodymium magnets are the strongest, and therefore also the most widely used. They are, among other things, used in hard disk drives (HDD), speakers, luminescence, wind turbines and hybrid electric motors. In the future it is expected that wind turbines and hybrid electric vehicles will be the largest applications, but HDD is the biggest today.

There are currently no program for end-of-life recovery or recycling of rare earth magnets (Öko-Institut, 2011). Many recycling processes have been reported, but none of them have been commercially developed due to bad yields, high costs and too low amounts of rare earths in the waste to make the recycling profitable (Oakdene Hollins, 2010). It has been concluded that the liquid metal extraction technologies are the most promising.

Japan is the only country in the world where there are some activity on the recycling of rare earth magnets, and only 1% is recycled (EPOW, 2011a). In the development of a green economy and technology in Europe, it is important to increase the amount of rare earths that is recycled.

1.2 Aim of work

This work had two main objects; to characterize magnetic waste and test recycling technologies.

Magnetic waste from WEEE Recycling AS was characterized, and two recycling technologies was examined; recovery of neodymium from Nd-Fe-B magnets by extraction using molten silver and extraction of neodymium by oxidation.

2   Theory

This chapter aims at explaining the theory at which the experimental work in this study is based on. It starts with an introduction to the Neodymium-Iron-Boron magnets and their applications. Further, the recycling of the magnets, as the situation is today, is explained. Finally, the previous work and theory behind the experimental work done in this study is presented.

Parts of this chapter are based on the authors previous project work the fall of 2011 (Bristøl, 2011)

2.1   Nd-Fe-B Permanent Magnets

Neodymium-Iron-Boron magnets are the strongest permanent magnetic material known (EPOW 2011), and they have many applications. From Figure 3 it can be seen that 31% of the magnets are used in hard disk drives today, and HDDs are thus the largest application of the magnets (EPOW, 2011). In the future it is expected that the biggest quantities of the magnets will be used in wind turbines and in high performance and light-weight motors in hybrid and electric vehicles (EPOW, 2011a).
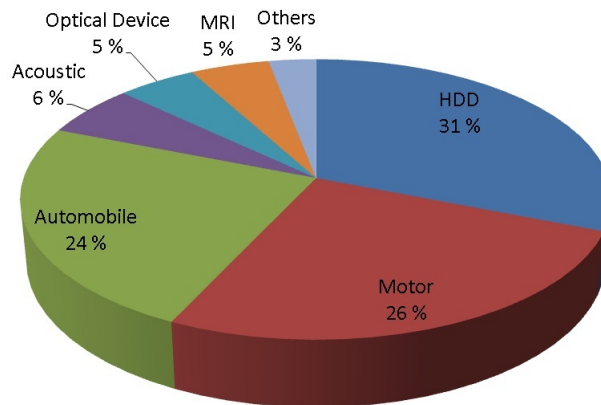
Figure 3: Applications of rare earth magnets (Bristøl, 2011)

The basic chemical formula of neodymium magnets is $Nd_2Fe_{14}B$, where Nd usually is a mixture of different rare earth elements (Öko-Institut, 2011). An estimation cited by EPOW (2011) states that the overall average rare earth content of a neodymium magnet is 69% neodymium, 23.4% praseodymium, 5% dysprosium, 2% gadolinium and 0.2% terbium.

The typical composition of neodymium-iron-boron magnets is 66wt% Fe, 29wt% Nd, 3wt% Dy and 1wt% B (Oakdene Hollins, 2010). Other metals

can be added to fine-tune the properties of the magnets for the different applications, such as cobalt, niobium, aluminum and gallium.

Dysprosium is added to the magnets in place of neodymium to improve the resistance to be demagnetized, the coercivity, and the temperature tolerance. Since terbium has a stronger influence on coercivity and lesser impact on remanence (the magnetization left after an external field is removed) than dysprosium, it would be a better additive to the magnets, but the supply of terbium is very limited and it is therefore expensive (Oakdene Hollins, 2010).

Didymium, a mixture of 75% neodymium and 25% praseodymium, is used in the magnets because praseodymium improves the corrosive resistance, and didymium is often cheaper than pure neodymium (Oakdene Hollins, 2010).

2.2 Nd-Fe-B Magnets in Electric and Electronic Equipment

Neodymium magnets are important in many components in different electric and electronic equipment, like laptop computers and smart phones (Öko-Institut, 2012). In laptop computers the magnets are found in the hard disk drives, the optical drive and in the loudspeakers. Figure 4 shows a picture of a dismantled hard disk drive, with the Nd-Fe-B magnets from the voice coil accelerator (Öko-Institut, 2012). There are at average 8.2 g of Nd-Fe-B magnets in laptop computers (Öko-Institut, 2012), which means that there are 2.14 g neodymium, 0.27 g praseodymium and 0.06 g dysprosium in one laptop computer. The amounts are considerably higher for desktop computers.
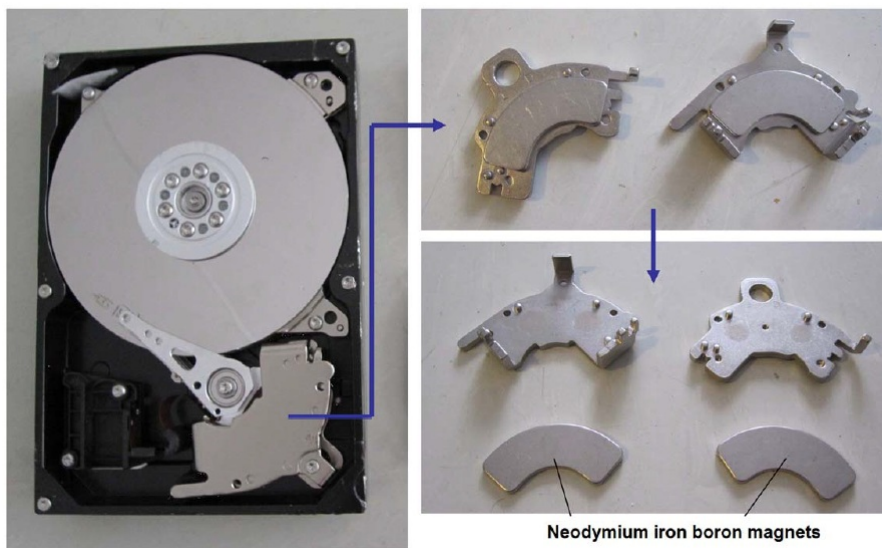
Figure 4: Nd-Fe-B magnet in voice coil accelerator in the hard disk drive (Öko-Institut, 2012)

Nd-Fe-B magnets are used in the loudspeakers in mobile phones, but there are no quantitative data available for the amounts of rare earths in these devices (Öko-Institut, 2012). A disassembled mobile phone and the Nd-Fe-B magnet from its loudspeaker is displayed in Figure 5.
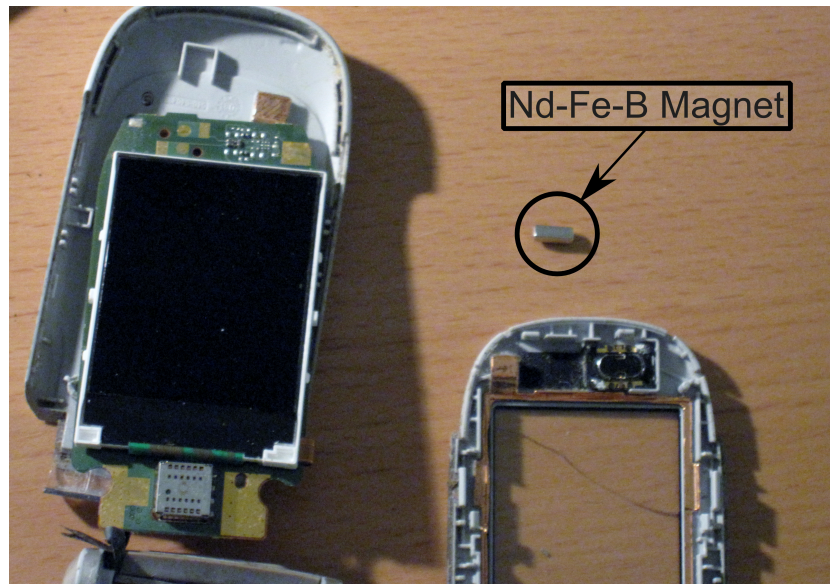
Figure 5: Nd-Fe-B magnet in cellphone

2.3   The Recycling of Nd-Fe-B Magnets

The neodymium magnets are fragile and brittle, and fracture easily (Oakdene Hollins, 2010 and EPOW, 2011a). Between 20% and 30% of the magnets are scrapped during manufacturing, hence there are big amounts of pre-consumer scrap as well as the post-consumer scrap.

As metioned in the introduction there are currently no commercial program for recycling or end-of-life recovery of rare earth magnets (Oakdene Hollins, 2010). All of the scrap materials are considered to be hazardous waste. The magnetic field generated by the magnets is to strong for air transportation, and the transportation of them are therefore restricted. Demagnetization is required before the magnets can be transported (Öko-Institut, 2011).

Nd-Fe-B magnets are not expected to enter the waste streams in large quantities for some time because the coercivity is good, and the products in which they are used in large amounts are durable (EPOW, 2011a). The number of hybrid and electric vehicles that are approaching end of life is still low, as well as for wind turbines, in which the installations have just begun. Recovery and recycling of magnets from vehicles is expected to become attractive in about 10 years, while the recycling from wind turbines is expected to take more than twice as long to become attractive. The magnets used in small electrical devices have already reached the waste streams, but the recovery is neither practical nor economical because of their size, and the fact

that they are glued to other components, so the separation is very difficult (EPOW, 2011). Today the magnetic materials in WEEE (waste electrical and electronic equipment) waste end up in light iron processing routes from which they can not be recovered.

It is believed that 300,000 tons of rare earth elements are trapped in WEEE waste streams in Japan today (EPOW, 2011a), and Japan is, as mentioned earlier, the only country in the world where there are some activity on recycling of rare earth magnets to date (Oakdene Hollins, 2010).

EPOW (2011a) quotes a report that concludes that the recycling of rare earth elements is both difficult and expensive because of the nature of the products and the dispersion of the materials, and less than 1% of rare earth elements are recycled from old scrap today.

Reuse of Nd-Fe-B magnets is suggested as an option, but it has turned out to be difficult. The properties and design of the magnets are often exactly specified for their original application. The magnets have to be used for the same type of product or their properties have to be changed through complex and expensive processes (EPOW, 2011a). Reuse does not occur today.

2.4   Recovery of Neodymium from Nd-Fe-B Magnets by Extraction using Molten Silver

Many methods for recovery of neodymium from Nd-Fe-B magnets have been examined (Bristøl, 2011). The variety of processes include molten salt processes exploiting chlorides (Oakdene Hollins, 2010), hydrometallurgical processes (Ellis et al. 1994), melt spinning (Itoh et al., 2004), glass slag method (Saito et al., 2003), electroslag refining (Ellis et al., 1994) and extraction technologies using molten silver (Takeda et al., 2004) and magnesium (Ellis et al., 1994, Oakdene Hollins, 2010 and Takeda et al., 2004). None of the methods have been commercially developed due to high costs and bad yields (Oakdene Hollins, 2010) and because the amounts of waste are not large enough (EPOW, 2011a). However, it has been concluded that the liquid metal extraction technologies are the most promising.

Takeda and co-workers (Takeda et al., 2004) were the first to exploit the recovery of neodymium by liquid-solid extraction with silver. The phase diagram of the silver-neodymium system (Wang et al., 2009) and the silver-iron system (Swartzendruber, 1984) are depicted in in Figure 6 a) and b), respectively. The phase diagram of silver and neodymium show that the two elements have high affinity to each other, and they form several intermetallics. Iron and neodymium, however, are immiscible at almost all temperatures and compositions. This is the reason why silver is suitable for the extraction of

neodymium from iron.
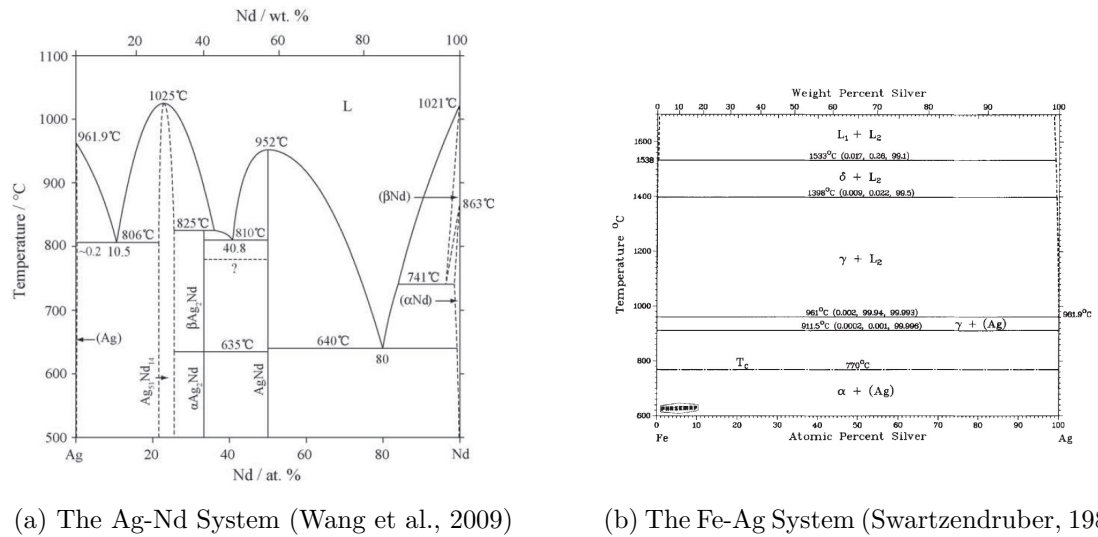
(a) The Ag-Nd System (Wang et al., 2009)   (b) The Fe-Ag System (Swartzendruber, 1984)

Figure 6: Phase Diagrams

Scrap chips with about 31 mass% neodymium was crushed and added into an iron crucible together with silver shots. The crucible was sealed with a lid by welding, and installed in a stainless steel vessel. An illustrative drawing of the apparatus is shown in Figure 7. The vessel was heated in an electric furnace at temperatures between 1000 and 1300ºC for 4 to 72 hours, and subsequently quenched in water.
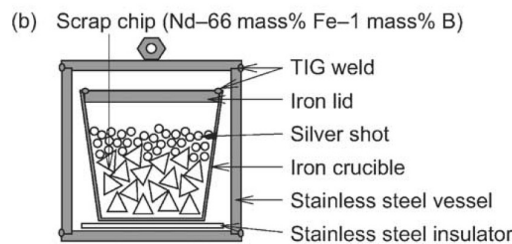
Figure 7: Illustrative drawing of the apparatus used by Takeda et al. (2004)

The scrap chips maintained their original shape after the heat treatment, and a Ag-Nd alloy was found in between the scrap chips. Figure 8 shows the cross section of a crucible after an extraction experiment. The white part is the scrap chips and the gray part is the Ag-Nd alloy.
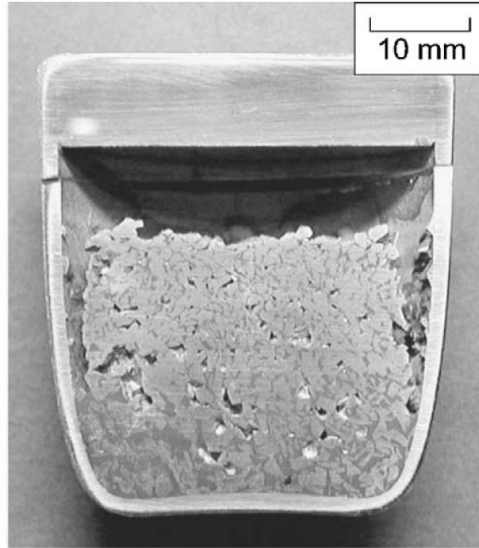
Figure 8: Cross section of crucible after extraction experiment (Takeda et al., 2004)

Figure 9 below shows a SEM image of the boundary between the scrap chips and the Ag-Nd alloy. Three phases can be observed. It was found by EDS that the black phase was pure iron, the gray phase was Ag-Nd alloy of the composition Ag:Nd=67:33, and the white phase was an alloy with the composition Ag:Nd=50:50. Takeda and his co-workers concluded that the gray phase was Ag_2Nd and that the white phase was $AgNd$.

The same figure also shows the neodymium concentration profile (the white line). The concentration of neodymium was significantly higher in the Ag-Nd alloy than in the scrap chips, and the neodymium concentration in the alloy was found to be 45-50 mass% at average.

11
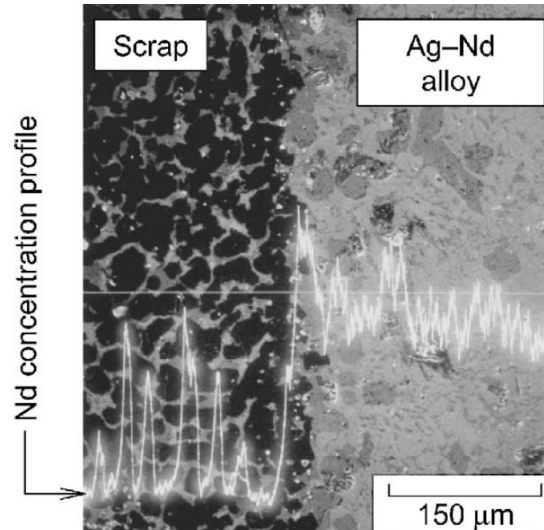
Figure 9: SEM picture of the interface between the Fe-phase and the Ag-Nd phase, with the Nd-concentration profile (Takeda et al., 2004)

It was found that more than 85% of the neodymium was extracted from the scrap into the Ag-Nd alloy after 4 hours at 1000ºC. The extraction ratio could be increased to about 90% when the holding time was increased to 72 hours.

Takeda and co-workers also performed the same experiments with master alloys without any boron, and the same results for extraction was obtained. Thus it could be concluded that the effect of boron on the extraction ratio could be disregarded.

2.5   The Nd-Fe-Ag Phase Diagram

To be able to understand the extraction process it is important to know something about how the elements in the system interact with each other. Since Takeda and his co-workers concluded that the boron does not have an effect on the extraction of neodymium from iron using silver, boron will be disregarded in this section (Takeda et al., 2004). The phase diagram of neodymium and iron is given in Figure 10 (SGTE, 2004). On the left hand side a blue line shows the composition of the alloy used in Nd-Fe-B magnets, assuming pure neodymium and no boron. When the alloy is heated to temperatures around 1000-1300º C, it consists of mainly $Fe_{17}Nd_2$. It is important to look for this phase in the extracted magnet scrap after an experiment.
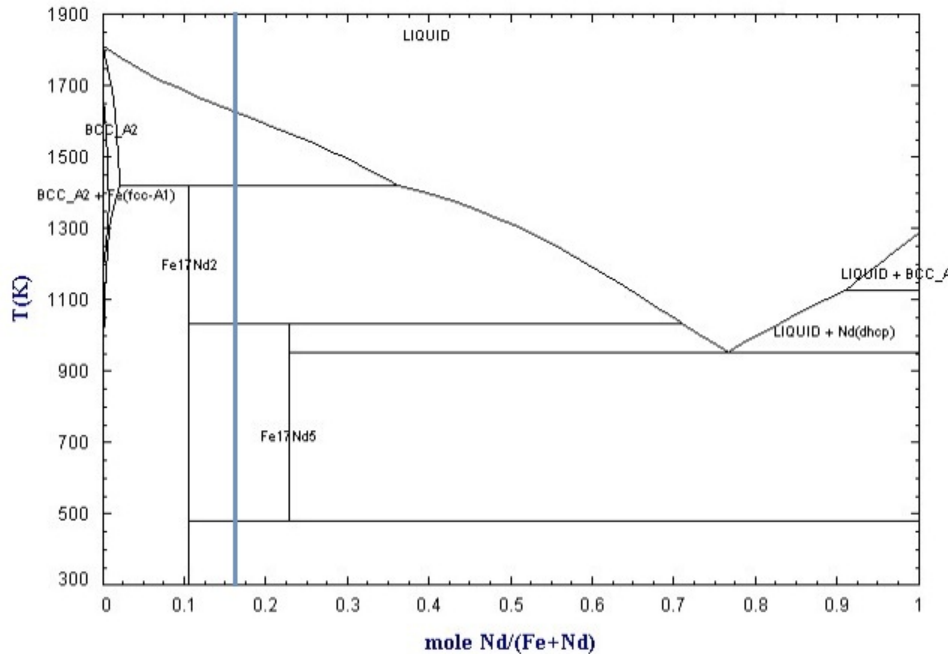
Figure 10: The Fe-Nd phase diagram showing the composition of the Nd-Fe-B magnet alloy (SGTE, 2004)

The Nd-Fe-Ag phase diagram at 1090º C is given i Figure 11 below (Raghavan, 2006). For an extraction experiment it is essential to have a mixture within the big two-phase field in the upper part of the phase diagram. In this phase field, two phases separates; one solid pure iron phase and

one liquid Ag-Nd alloy. When the sample is cooled down, these two phases will remain separated because of neodymium's strong affinity to silver.
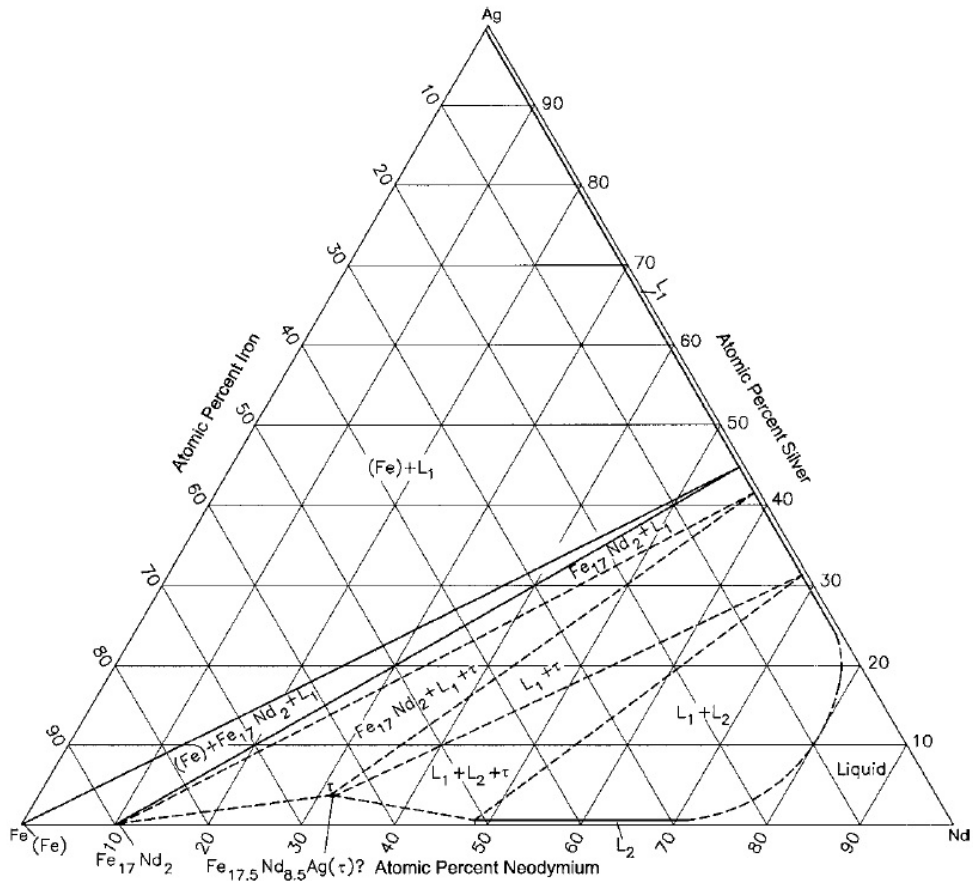
Figure 11: The Nd-Fe-Ag phase diagram at 1090°C (Raghavan, 2006)

2.6 Extraction of Neodymium by Oxidation

The rare earth elements form very stable oxides, and neodymium is no exception (Gupta & Krishnamurthy, 2005). The standard Gibbs energy of formation of neodymium oxide is $\Delta G^0_{Nd_2O_3} = -1720.8\,kJ/mol$ (CRC, 2011). Iron has two different oxidation states, Fe^{2+} and Fe^{3+}, and forms three different oxides, FeO, Fe_2O_3 and Fe_3O_4 (Zumdahl, 2005). The standard Gibbs energy of formation of the three forms of iron oxide is $\triangle G^0_{FeO} = -251\,kJ/mol$ (SI Chemical Data, 2002), $\triangle G^0_{Fe_2O_3} = -742.2\,kJ/mol$ and $\triangle G^0_{Fe_3O_4} = -1015.4\,kJ/mol$ (CRC, 2011), and for boron oxide it is $\Delta G^0_{B_2O_3} = -1194.3\,kJ/mol$ (CRC, 2011). The more negative the Gibbs energy of formation is, the more stable is the oxide (Stølen & Grande, 2004). This means, thermodynamically, that in a mixture of neodymium, iron and boron, neodymium will be oxidized first. This could might be used in a procedure for recovery of neodymium from Nd-Fe-B magnets.

The Ellingham diagram can be used to find the oxygen partial pressure in which iron oxide and oxygen is in equilibrium. If the oxygen partial pressure is lower that the equilibrium partial pressure, oxidation will not occur (Stølen & Grande, 2004). The Ellingham diagram showing the different equilibrium partial oxygen pressures at 1300°C is depicted in Figure 12.

Another feature of the Ellingham diagram is that the relative stability of the oxides can be determined by the position of their lines in the diagram. The closer to the top of the diagram the line is, the less stable is the oxide and the probability of the formation of it (Stølen & Grande, 2004). From this it can be seen from Figure 12 that the order of stability of the iron oxides is $FeO > Fe_3O_4 > Fe_2O_3$. To prevent oxidation of iron in an experiment with the aim of oxidizing neodymium, the oxygen partial pressure should be below the equilibrium partial pressure for FeO at the relevant temperature. For 1300°C the oxygen partial pressure should be below 10^{-12}atm, as seen from the figure.

15
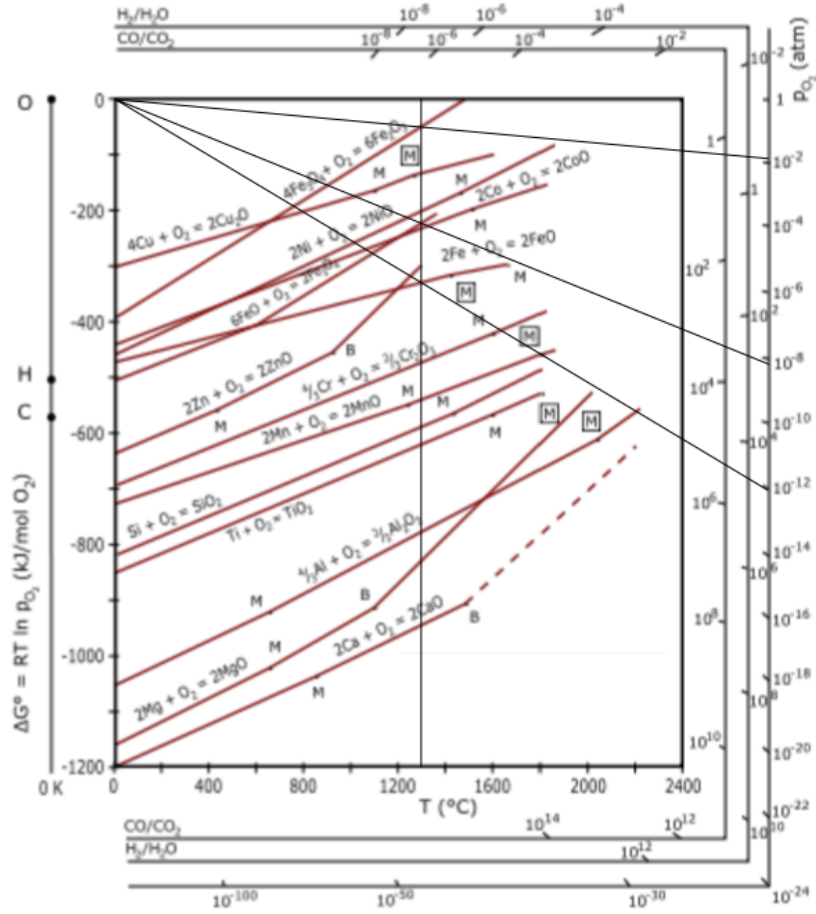
Figure 12: The Ellingham diagram showing the equilibrium oxygen partial pressures for iron oxide at 1300ºC

3 Experimental

This chapter intends to explain the experimental methods investigated in this study. Three types of experiments have been done; characterization of magnetic waste, extraction of neodymium using molten silver and extraction of neodymium through oxidation.

3.1 Characterization of Magnetic Waste

In this section the characterization of waste from a WEEE recycling facility is described. This was done to find out whether there are considerable amounts of rare earth elements in the waste or not. This information is a key to find out whether recycling of rare earth magnets will be profitable, now or in the future.

3.1.1 Materials

The materials used in this part of the study are magnetic waste from WEEE Recycling AS. The company processes electric and electronic waste like white goods, cooling devices, TVs and miscellaneous electronic equipment (WEEE Recycling AS, 2011). The magnets from the different equipment gets stuck everywhere in the machinery and have to be scraped off to prevent clogging. This is the only way to collect the magnetic scrap with today's technology.

A picture of the sample is depicted in Figure 13. As seen from the picture, the sample was very inhomogeneous and contained a combination of magnetic powder, magnet pieces and other non-magnetic objects like screws and pieces of plastic.

Figure 13: Magnetic Waste from WEEE Recycling AS (Bristøl, 2011)

3.1.2   Method

To be able to do an analysis of the material, the different components had to be separated and sorted. A visual examination of the different components lead to sorting in four different piles; strong magnets, weak magnets, magnetic powder and non-magnetic components.

The magnetic powder was pulverized and percolated to a fine dust with particle size around $75 \mu m$. The magnets, both strong and weak, were cleaned to get a pure surface. The different metal pieces could easily be dismantled, but the dust was hard to separate from the strongest magnets. The different piles were analyzed as described in the following section.

The sample and the different piles of components were also photographed and weighted.

3.1.3 Analysis

Both the magnetic powder and the strong and weak magnets were analyzed by X-ray fluorescence (XRF). In an XRF analysis the sample is bombarded with high energy electrons (West, 2010). This results in the sample emitting characteristic X-rays, which in turn are detected. Different elements have their own characteristic X-ray emission spectrum, and XRF can therefore be used for elemental analysis.

Magnetic powder The magnetic powder was analyzed by XRF. Four samples was taken out and pressed into pellets before analysis.

A semi-quantitative program, without standards, on a BRUKER S8 Tiger 4 kW X-ray spectrometer was used.

Magnets The magnets, both strong and weak, were analyzed with a portable XRF. Four examples from each of the two piles were taken out to be analyzed. A program for electronic alloys was used on a Thermo Scientific, Niton XL3t XRF analyzer.

3.2 Extraction of Neodymium Using Molten Silver

In this part of the study a reproduction of the work done by Takeda and his co-workers (Takeda et al., 2004) was attempted. Magnets and silver were loaded into stainless steel containers and heated to 1000-1250º C in a heat resistance furnace for 4-5.5 hours.

It was planned to do a separation of neodymium and silver by reacting the neodymium with carbon to form neodymium carbide. This was not done because the resulting Fe-B phase and Ag-Nd alloy were hard to separate.

3.2.1 Materials

The magnets used in this study was commercial Neodymium-Iron-Boron discs with a Nickel coating.

The silver used was granulated and of a purity of 99.9 %.

3.2.2 Setup

The containers used in this study were made of 316 stainless steel. They were gas tight and had a gasket of the same stainless steel. The containers were cylindrical with a length of about 4.5 cm (6 cm with the screw cap) and a diameter of about 4 cm. A picture of the container is shown in Figure 14.

Figure 14: Picture of the Stainless Steel Container used

The containers were filled inside a glove box with argon atmosphere containing about 5 ppm oxygen and 7 ppm water.

The actual experiments were performed in a heat resistance furnace at temperatures between 1000-1250º C.

3.2.3   Method

The magnets and silver where filled into gas tight stainless steel containers. Introduction of oxygen to the system would probably result in oxidation of neodymium, and thus the filling of the containers was done in a glove box with an argon atmosphere.

Five experiments was carried out, and two different compositions were used. For the four first experiments a Ag:Nd ratio of 5:1 by weight was used, and for the fifth experiment a Ag:Nd ratio of 10:1 by weight was used. The compositions are shown in the Ag-Fe-Nd phase diagram depicted in Figure 15.
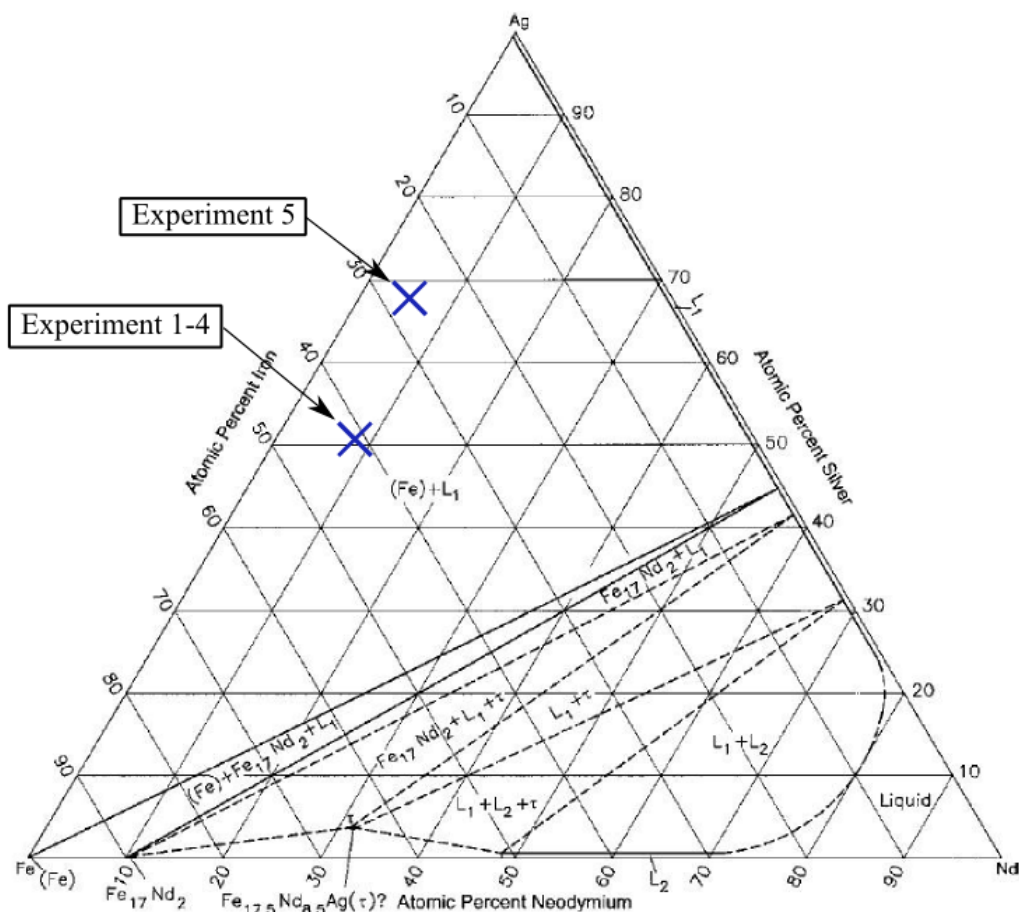
Figure 15: The composition used in the extraction experiments

The weights of magnets and silver used in the different experiments, and the calculated atomic percentages are shown in Table 8 in Appendix 1.

The different experiments were conducted at different temperatures for varying time. Some of the mixtures were even heated several times. An overview of the different temperatures and times is given in Table 1.

The magnets in experiment 1 and 2 were loaded into the container unbroken, and in the rest of the experiments the magnets were divided into smaller pieces.

3.2.4 Analysis

After the experiments was done, the containers were sectioned, and slices with a thickness of about 5 mm were cut off. These slices were subsequently grinded to get a smooth surface before the analysis.

Table 1: Temperatures and Times used in the Experiments

Experiment	Temperature [ºC]	Time [min]
1	1000	225
2	1100	255
	1170	318
3	1000	260
	1100	251
	1260	292
4	1170	305
5	1250	251

The samples were analyzed by energy-dispersive spectroscopy (EDS) in a scanning electron microscope (SEM). A Hitachi SU-6600 FESEM was used with a beam voltage of 20 kV, work distance of about 10 mm and a magnification of 300. An automatic PB-ZAF program was used for quantification.

3.3   Extraction of Neodymium by Oxidation

In lack of profitable recycling technologies, new methods have to be developed. This part of the experimental study investigate the possibility of extracting neodymium directly from the Nd-Fe-B alloy by oxidation.

3.3.1   Materials

The same Nd-Fe-B magnets were used in this experiment as in the previous section.

Iron flakes were added to the magnets pieces.

3.3.2   Setup

Graphite crucibles, 7 cm in height and 3.6 cm in diameter, were filled with pieces of magnets and iron, and heated in a Graphite tube resistance furnace. A schematic drawing of the furnace is given in Figure 16.

A resistance furnace is heated by passing a current through a resistor, in this case graphite, to form a thermal power (Motzfeldt, 2004). The power generated can be expressed by the following expression: $W = RI^2$, where W is the thermal power, R is the resistance of the resistor and I is the current. The resistor is connected to an electric power supply in both ends. The benefit of using a resistance furnace is accurate temperature control both in terms of temperature uniformity and constancy in time.

22

a – Gas inlet valve
b – Heat shield
c – Graphite heating element
d – Molybdenum/graphite crucible holder
e – Crucible with sample
f – Thermocouple with alumina tube, side
g – Gas outlet valve
h – Molybdenum rod, sample holder
i – Thermocouple with alumina tube, bottom
j – Vacuum valve
k – Air inlet valve
l – Water cooling tubes
m – Pulling
n – Copper cup
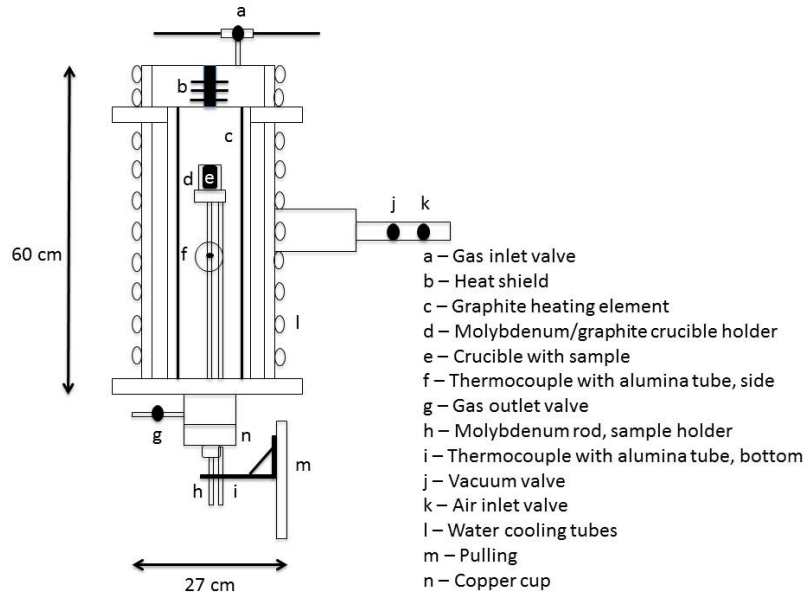
Figure 16: Schematic drawing of the Graphite tube resistance furnace

3.3.3 Method

Iron and pieces of Nd-Fe-B magnets were loaded into the crucible with a Fe:Nd ratio of 5:1 by mass. Two experiments were carried out and the weight of materials used, as well as the molar fractions from the experiments, are given Table 11 in Appendix 2. The composition of the experiments are shown in the phase diagram in Figure 17.
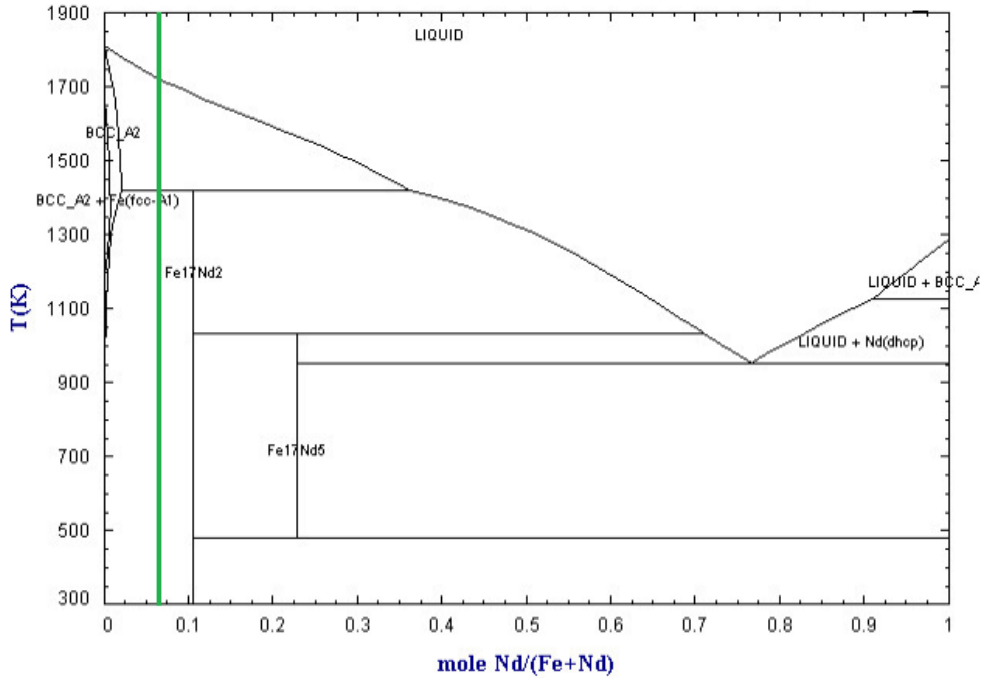
Figure 17: The composition used in the oxidation experiments

The samples were heated to about 1350ºC in a graphite tube resistance furnace.

The furnace was filled with argon gas of purity 99.99% and an oxygen content of 5 ppm or less , and the same gas was flowing through the furnace during the experiment. An oxygen content of 5 ppm is equal 0.0005%, which at atmospheric pressure, which was used in the experiment, correspond to an oxygen partial pressure of $5 \cdot 10^{-6}$ atm.

3.3.4   Analysis

The crucibles were cut and grinded like the samples from the previous section.

The samples were analyzed by energy-dispersive spectroscopy (EDS) in a scanning electron microscope (SEM). As in the preveous section a Hitachi SU-6600 FESEM was used with a beam voltage of 20 kV, working distance of 10 mm and magnification of 300. An automatic PB-ZAF program with correction for oxides was used

24

4 Results

This chapter is meant to summarize the results obtained in the experiments conducted in the study. Some limited explanations of the results are given, but the main discussion is presented in chapter 5.

4.1 Characterization of Magnetic Waste

As described in section 3.1 the sample was dismantled and sorted into four piles. Figure 18 displays photos of the these piles.

(a) Strong Magnets

(b) Weak Magnets

(c) Magnetic Powder

(d) Non-magnetic Components

Figure 18: The magnetic waste was divided into four piles

Table 2 below shows the weight of the sample and the different piles. The different pile's percentage share of the total weight have been calculated, and are also given in the table.

Table 2: Weight of the different piles

Component	Weight [g]	Percentage share
Strong magnets	440 ± 1	17 %
Weak magnets	1542 ± 1	60 %
Magnetic powder	533 ± 1	21 %
Non-magnetic components	65 ± 1	2 %
Total	2580 ± 10	100 %

Figure 19: Average values from the XRF analysis of the magnetic powder

4.1.1   Magnetic Powder

The measured values from the XRF analysis of the powder are given in Table 12 in Appendix 3 at the end of the report. All the samples contain the same compounds, with a few exceptions, and they show the same trends regarding the amounts. In Figures 19 and 20 are the average values from the analysis plotted. All the compounds found are plotted in Figure 19, while the compounds with low concentrations are plotted again in Figure 20 for to make it easier to see the relative amounts.

As seen from the figures, are silicon-, iron-, magnesium-, calsium- and aluminum oxides the main constituents in the magnetic powder.

The main aim of this work has been to find out whether there are consid-
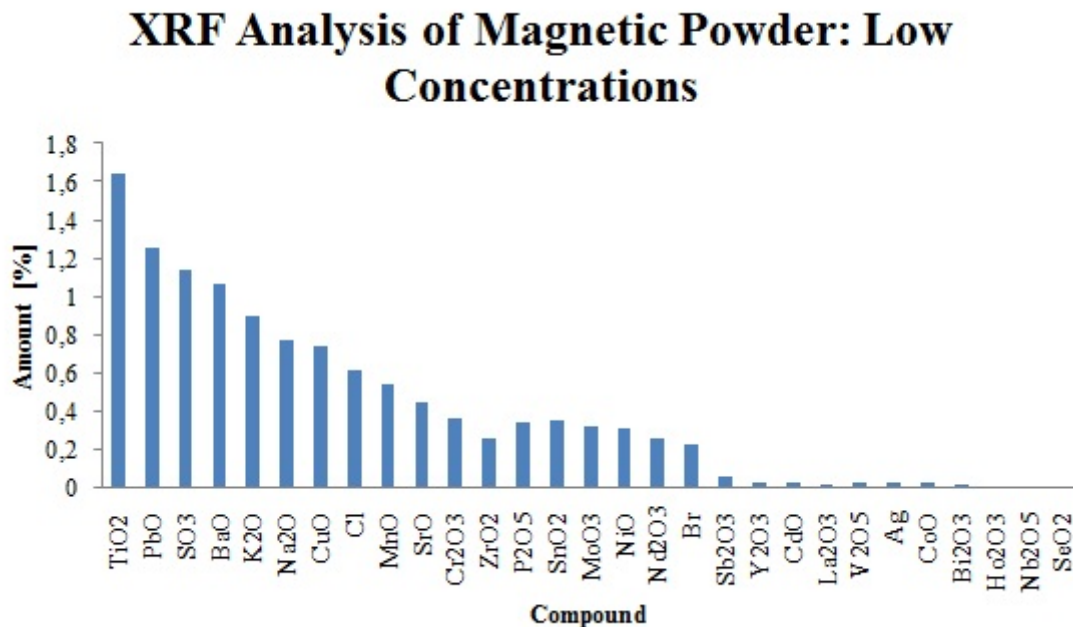
Figure 20: The average values of the components with low concentrations from the XRF analysis of magnetic powder

erable amounts of rare earth elements in the magnetic waste. The amounts of rare earth elements detected in the analysis of the magnetic powder are shown in Figure 21 below. Four rare earth elements were found in the powder; neodymium, yttrium, lanthanum and holmium. They were all found at concentrations below 0.3 %.

As seen from Table 12 in Appendix 3, the numbers do not sum up to 100 %, and it is probable that the samples contained some compounds that the XRF detector was not able to detect.

4.1.2   Magnets

The raw data from the analysis are given in Table 13 for the strong magnets and 14 for the weak magnets in Appendix 4. The numbers are given in percent of the area analyzed, and the analysis is hence a spot check of the surface. For simplicity it has been chosen to focus on the elements that constitute most of the magnets, namely elements that have been measured to constitute more than 0.09 %.

The results for the strong magnets are given in Table 3. The error has not been included in the sum. The numbers for platinum and gold are provided
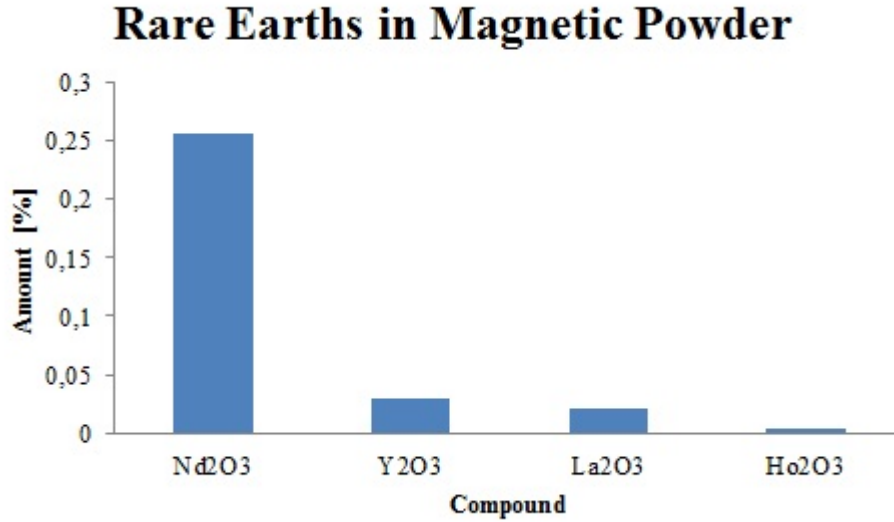
Figure 21: Rare earth elements in the magnetic powder

because of the high values for magnet number 4.

Table 3: The result of the analysis of the strong magnets

Element	Magnet 1 [%]	Magnet 2 [%]	Magnet 3[%]	Magnet 4 [%]
Ni	72.291 ± 0.381	88.307 ± 0.48	92.533 ± 0.46	0.133 ± 0.02
Fe	25.661 ± 0.107	7.288 ± 0.083	3.834 ± 0.057	93.416 ± 0.098
Hf	0.672 ± 0.033	0.916 ± 0.05	1.163 ± 0.052	0.36 ± 0.029
Co	0.733 ± 0.041	0.806 ± 0.033	0.194 ± 0.023	0.157 ± 0.059
Pb	0.406 ± 0.015	0.501 ± 0.023	0.642 ± 0.024	0 ± 0.009
Mn	0.07 ± 0.012	0.958 ± 0.025	0.474 ± 0.018	0.271 ± 0.023
Ag	0 ± 0.009	0.424 ± 0.01	0.449 ± 0.01	0 ± 0.009
Cr	0.005 ± 0.002	0.255 ± 0.004	0.087 ± 0.002	0.221 ± 0.003
Au	0 ± 0.03	0 ± 0.047	0 ± 0.046	3.92 ± 0.052
Pt	0 ± 0.379	0 ± 0.563	0 ± 0.589	1.348 ± 0.047
SUM	99.838	99.455	99.376	99.826

A picture of one of the strong magnets that were analyzed is shown in Figure 22 below. The composition and appearance are both important factors to consider when determining what material the magnets are made of.

The results for the weak magnets are given in Table 4. Again, the error has not been included in the sum.

Figure 23 depicts one of the weak magnets that was analyzed in this study.

28
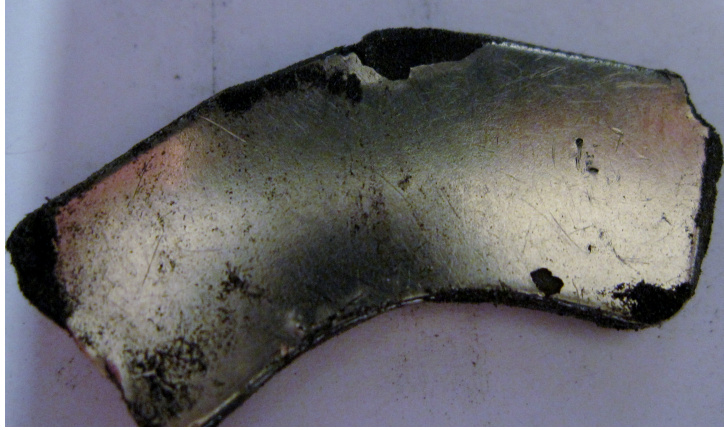
Figure 22: Picture of one of the strong magnets that were analyzed in the study

Table 4: The results of the analysis of the weak magnets

Element	Magnet 1 [%]	Magnet 2 [%]	Magnet 3[%]	Magnet [%]
Fe	95.688 ± 0.107	95.268 ± 0.093	96.712 ± 0.152	94.843 ± 0.051
Zr	2.253 ± 0.01	2.123 ± 0.018	2.292 ± 0.032	2.108 ± 0.01
Ba	0.248 ± 0.006	0.759 ± 0.013	0.197 ± 0.016	1.355 ± 0.009
Mn	0.41 ± 0.014	0.329 ± 0.026	0.246 ± 0.041	0.387 ± 0.015
Ni	0.292 ± 0.016	0.288 ± 0.03	0.227 ± 0.05	0.292 ± 0.017
Ta	0.241 ± 0.019	0.164 ± 0.036	0 ± 0.115	0.205 ± 0.019
Co	0.272 ± 0.036	0 ± 0.132	0 ± 0.22	0.251 ± 0.037
SUM	99.404	98.931	99.674	99.441

Figure 23: Picture of one of the weak magnets that was analyzed in the study

4.2   Extraction of Neodymium Using Molten Silver

The cross sections of two of the containers from the experiments are shown in Figure 24. Sub figure a) shows the cross section of a container where the magnets were loaded into it in one piece, while sub figure b) shows a cross section of a container where several pieces of magnets were used.
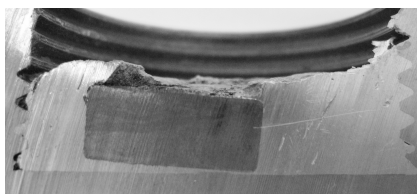
(a) Container with whole magnet
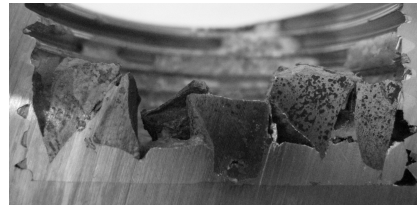
(b) Container with magnet pieces

Figure 24: The cross section of two of the crucibles used

The samples from the extraction experiments were analyzed by EDS in a SEM. Two phases were observed in all of the samples; one grey and one black. Figure 25 shows a typical picture of the interface between the two phases. Table 9 and 10 in Appendix 1 summarizes representative results from each sample.

The grey phase consisted of mainly silver and neodymium and the black phase consisted of mainly iron with some nickel. The content of neodymium and silver in the grey phase is plotted in Figure 26, and the iron and nickel
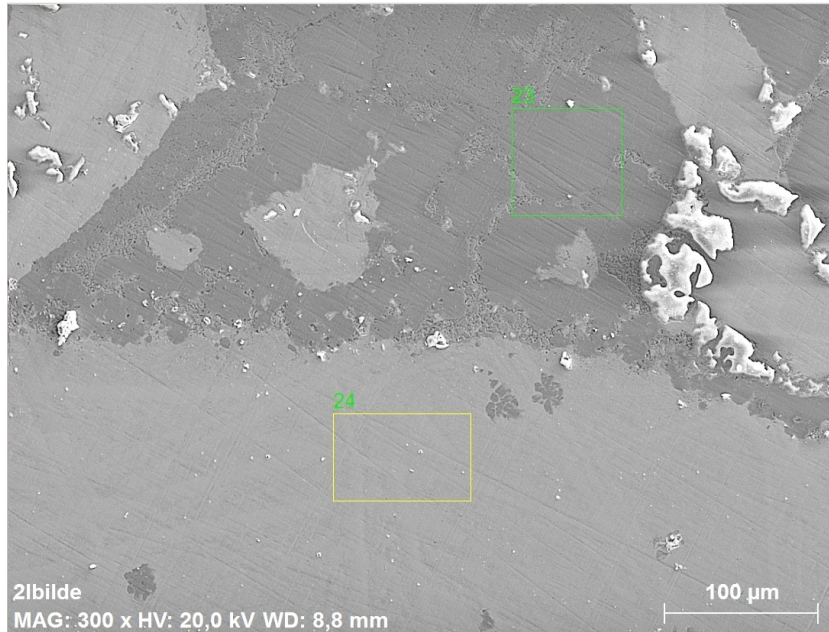
Figure 25: SEM picture of the interface between the grey and the black phases

content are plotted in Figure 27.

It can be seen from the figures that the extraction had different results for the different experiments. There can be several reasons for that, which will be discussed in section 5.2.

4.3 Extraction of Neodymium by Oxidation

A cross section of the crucible after one of the experiments is shown in Figure 28. Two different phases can be seen; one bulk phase, and some rectangular brighter phases. Both crucibles had the same appearance after the experiment.

A SEM picture of the interface between the two phases is depicted in Figure 29. The bright phase seems to be smoother than the other phase. The two rings in the picture shows the area where the EDS analysis was done. An automatic PB-ZAF program both with and without correction for oxides were used, and the results are given in Table 5.

Both results shows that there are mostly iron in the smooth bright phase and some neodymium or neodymium oxide in addition to a lot of iron in the non-smooth darker phase. The values for neodymium and neodymium oxide is lower than expected.

Silver and Neodymium content in grey phase
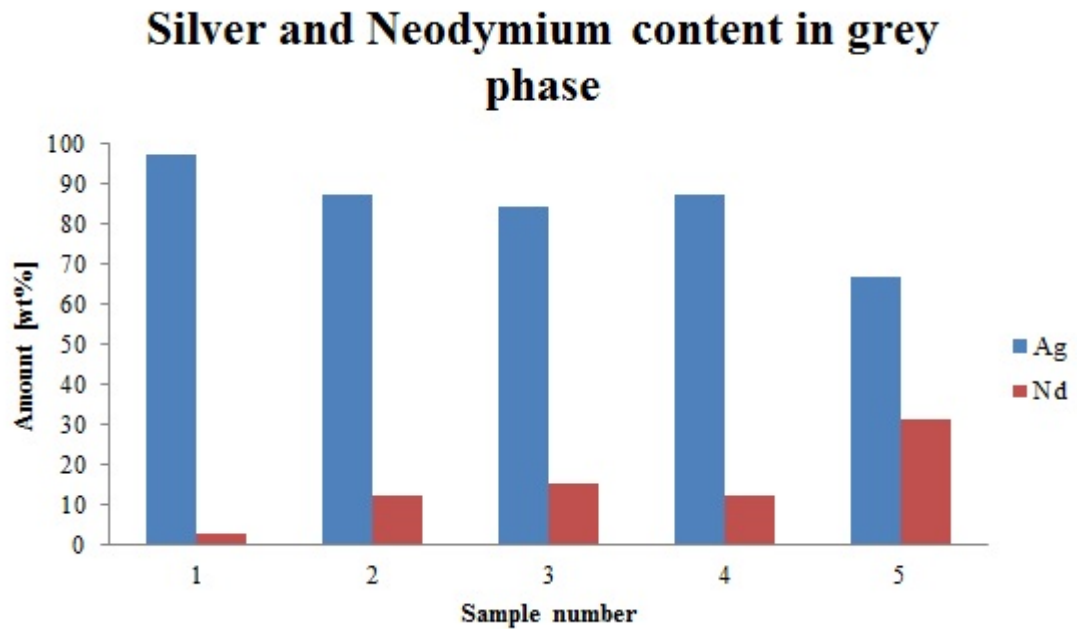
Figure 26: Silver and neodymium content in the grey phase

Iron and Nickel content in black phase
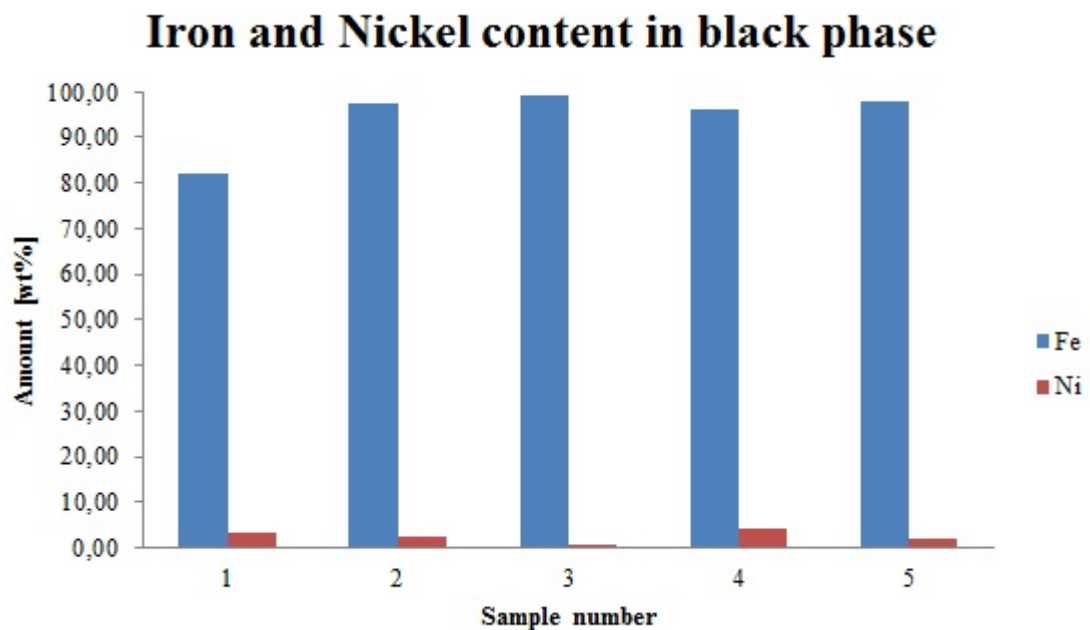
Figure 27: Iron and nickel content in the black phase
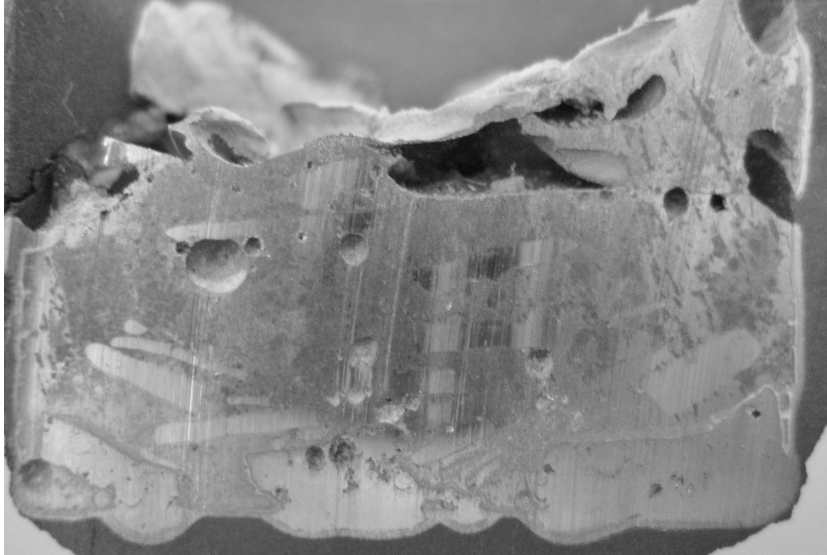
Figure 28: Cross section of a crucible after an experiment

Figure 29: SEM picture of the interface between the two phases in the oxidation experiment

Table 5: Results from the EDS analysis

Compound	Smooth Phase [wt%]	Non-smooth Phase [wt%]
FeO	99.71 ± 2.19	93.01 ± 1.85
NiO	0	0.93 ± 0.04
Nd_2O_3	0.29 ± 0.03	6.06 ± 0.16
O	0.27 ± 0.06	2.04 ± 0.23
Fe	99.73 ± 2.47	91.86 ± 2.05
Ni	0	0.70 ± 0.04
Nd	0	5.39 ± 0.15
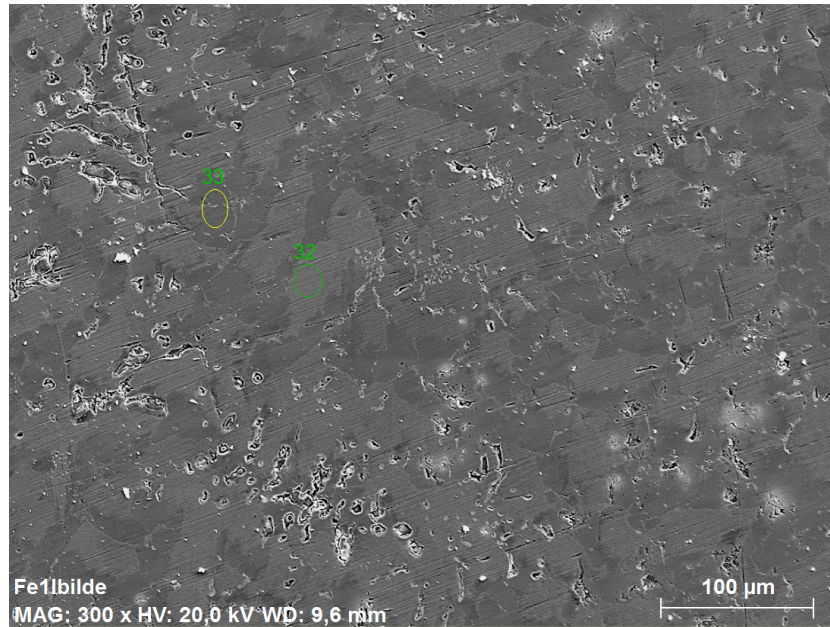
Figure 30: Representative picture of the microstructure

Throughout the samples, two phases could be seen in the SEM pictures; one dark phase and one light phase. A representative picture of the microstucture is given in Figure 30.

The content of the phases was pretty unequal for the two samples, as can be seen from the values given in Table 6. These areas were also analyzed by both programs mentioned above. The analysis within the same area in the same phase with the two programs show some inconsistency, for instance the light phase in sample 2 was calculated to a much higher weight percent neodymium oxide than neodymium. It is also worth noticing that almost no neodymium was detected in sample 1.

Table 6: Result from EDS analysis of the grey and the black phase

| Compound | Sample 1 | | Sample 2 | |
	Dark phase[wt%]	Light phase[wt%]	Dark phase[wt%]	Light phase[wt%]
FeO	99.08 ± 2.05	100 ± 2.09	94.32 ± 1.96	81.18 ± 1.39
NiO	0	0	0	0.81 ± 0.04
Nd_2O_3	0.92 ± 0.05	0	2.40 ± 0.08	18.01 ± 0.36
O	0	0.09 ± 0.04	2.54 ± 0.28	2.54 ± 0.28
Fe	99.3 ± 2.3	99.25 ± 2.39	95.13 ± 2.16	95.13 ± 2.16
Ni	0.37 ± 0.03	0.66 ± 0.04	0.59 ± 0.04	0.59 ± 0.04
Nd	0.32 ± 0.03	0	1.73 ± 0.06	1.73 ± 0.06

5   Discussion

5.1   Characterization of Magnetic Waste

The analysis of the magnetic powder was done with a semi-quantitative program without standards, thus the numbers obtained in the analysis are not entirely reliable. In stead they should be regarded as an indication on what compounds that are present, and at what relative amounts.

As mentioned before, the values measured does not sum up to 100 %. There could be several reasons for that. One possible reason is that the powder can contain elements that the instrument is not able to detect. As an example is the instrument not able to detect carbon (Sørløkk, 2012), which it is possible that the sample contains. Another possible reason why the numbers does not add to 100 % is that a semi-quantitative program without standards was used, hence there are no reference to compare the results with.

As seen from Figure 19 above, the magnetic powder mainly consist of silicon-, iron-, magnesium-, calcium- and aluminum oxides. These are all common metals, and it is not surprising to find them in relatively big amounts in waste from electric and electronic equipment.

The amounts of rare earth elements in the magnetic powder are very low. The four rare earth oxides together make up at average 0.3111 % of the samples. Assuming that all elements are evenly distributed this means that there are about 1.66g rare earth oxides in the magnetic powder, where 1.36g out of it is neodymium oxide. The amount of rare earth elements is even lower. This result indicates that recovery of rare earth elements from the magnetic powder will not be profitable, unless there are very big amounts of powder available.

The numbers from the XRF analysis of the magnets shows big uncertainty for some elements, whereas for other elements the uncertainty is very low.

From the analysis of the strong magnets it can be seen that the three first magnets have similar composition, while the composition of the fourth magnets stands out. This indicates that the three first magnets could consist of the same material, while the fourth probably is something else.

Comparing the picture in Figure 18 (a) and 22 with Figure 4 in section 2.2, several of the strong magnets look like the magnets used in hard disk drives. All the three first strong magnets that were analyzed contained big amounts of nickel and iron. This is in agreement with the expectations for Nd-Fe-B magnets since they usually are nickel-coated and their main constituent is iron. Many of the other elements that were detected, however, is fairly surprising. Hafnium is used in some metal alloys to enhance the corrosion

resistance, and in microprocessors. So, the hafnium in the sample may be contamination from other components in the equipment, or it can have been added to prevent corrosion. Hafnium was not detected in the analysis of the powder, which suggest that the hafnium is intentionally added to the alloy.

Cobalt is an important component in other rare earth magnets (Oakdene Hollins, 2010), and may stem from other magnets. Small amounts of cobalt was also detected in the XRF analysis of the magnetic powder. Lead, manganese and chromium was detected in the magnetic powder, and the relatively high content of them on the magnets may be due to remaining powder on the surface. This may also be the case for silver.

Neodymium was not detected, and it is believed that it is because of the limitations of the equipment; that neodymium can not be detected by the detector used.

Based on the appearance of strong magnets 1-3 and their magnetic strength, combined with the high levels of iron and nickel it is believed that they are Nd-Fe-B magnets. Strong magnet number four is believed to be something else. This means, if it is assumed that all of the other strong magnets are Nd-Fe-B magnets, that about 17 % of the magnetic waste is Nd-Fe-B magnets. From section 2.1 it is known that the magnets contain 32 wt% rare earth elements, which means that there are about 140g rare earth elements in the strong magnets.

As seen from Table 4 the weak magnets contain mainly iron with some small amounts of zirconium, barium and manganese. These elements are in accordance with the content of ferrite magnets (West, 2010).

In total this means that in the sample of magnetic waste there was less than 142g, or 5.5 %, of rare earth elements. This indicates that the recovery of rare earth elements from the magnetic waste is not profitable today. In the future, when more rare earth elements enter the waste streams (EPOW, 2011a), and if the technology for recycling and separation of the magnets have been developed, it might be profitable.

As mentioned briefly above and in previous work (Bristøl, 2011), the characterization of the magnetic waste was hard. The biggest challenge being the fact that it is permanently magnetic, which makes it impossible to characterize by common methods. The method used may not be the best either. In the analysis of the powder there are not any references for comparison and it can not be determined whether there are other elements that were not detected in the sample. In addition some of the numbers in the analysis of the magnets shows large values for uncertainty.

It should also be mentioned that only one sample has been examined, and it is therefore impossible to know if the numbers obtained are representative for the magnetic waste or not. In addition there are no numbers for how

much Nd-Fe-B magnets that enter the waste stream compared to how much that is collected from the machinery. Technologies for separation of the magnets from other components should be developed to make the recycling as profitable as possible.

5.2 Extraction of Neodymium Using Molten Silver

From Figure 24 it can be seen that the magnets retained their shape, both those that were loaded into the container in one piece and those that were cut into pieces. This is in accordance with the work of Takeda and his co-workers (Takeda et al., 2004) as described in section 2.4.

In the picture in Figure 25 the two phases can easily be observed, but they look somewhat different than the the picture in Figure 9, from previous work. First of all it is worth noticing that only one grey phase can be observed in the picture from this study, compared to two phases in the previous study. Secondly, Figure 25 depicts a solid black phase compared to the more blotchy phase in Figure 9. This indicates that the experiments have proceeded, in some degree, differently on the atomic level. This can be due to different materials, apparatus or procedure. Which one it is, and to what degree is hard to determine.

Like in the work of Takeda et al. the grey phase contains silver and neodymium, while the black phase contains principally iron, with some contamination of nickel, probably from the coating. However the different samples have varying compositions in the grey phase. From sample 1 to 3 it seems like the neodymium content increases with extraction temperature and time, but then it decreases in sample 4, against the trend. The reason is probably that sample 2 and 3 were heated several times, leading to a longer extraction time in total. The result in experiment 5 indicates again that the neodymium content is increased with temperature, and that a higher Ag:Nd ratio enhance the effect or extraction rate.

Very small amounts of neodymium was found in the black phase of sample 1, even though there are small amounts in the gray phase. In the other experiments no neodymium is detected in the black phase, but different amounts are extracted into the silver. These odd results indicates that the measurement is not fully satisfactory. One of the reasons can be that neodymium is a heavy element with high energy electrons. It takes more energy to kick out an electron in neodymium than in iron, silver or nickel. This leads to the use of lower energy electrons (i.e. electrons from shells further away from the nucleus) for detection of neodymium. The signals from these lower energy electrons may overlap with the signals from electrons from the other elements, and the equipment can be fooled to think that the neodymium is

another element.

In some parts of the samples it was hard to find any neodymium at all. This, combined with the low amounts of neodymium measured in total, can be explained by neodymium not being evenly distributed in the samples.

The neodymium content is higher in the Ag-Nd alloys explained in Takeda et. al (2004) than in the results given in this report. This might be due to the reasons explained above or other reasons. One possible reason could be different magnet:silver ratio, since no mixing ratio is explained in the work by Takeda and co-workers.

The results presented in section 4.2 all in all shows that neodymium was extracted from the Nd-Fe-B magnets in to the silver, but they do not give a clear answer to what extent the neodymium was extracted. Maybe another method of analysis could give a clearer answer.

5.3   Extraction of Neodymium by Oxidation

From Table 5 it can be seen that the smooth phase from Figure 29 contains iron or iron oxide, while the non-smooth phase contains mostly iron or iron oxide and some neodymium or neodymium oxide, with some contamination of nickel, probably from the magnet coating. The weight percent of neodymium is lower that what is expected from the weight percents calculated in Table 11 in Appendix 2. There are several possible reason for that. One reason can be that the neodymium exists partly, or totally, as oxide. Another reason is that it might not be evenly distributed in the sample, and finally it can be because of the reasons discussed in the previous section; namely that neodymium could have been hard to detect.

Also, since both the metal and the oxide phases can be detected for iron and neodymium, it is hard to say something about what phases that actually are present. When considering the oxygen content of the argon gas used, it is possible that some of the iron have been oxidized in addition to the neodymium.

As mentioned briefly in section 4.3 there is some inconsistency in the results measured by the two different analysis programs for the same areas, especially for the light phase in sample 2. This could be due to the problems with detecting neodymium that have been described earlier. It can also mean that all the neodymium found in the analysis are present as neodymium oxide.

Almost no neodymium was detected in sample 1. This can also be due to the reason described earlier, i.e. unevenly distributed neodymium in the sample and that it is hard to detect neodymium.

The aim of these experiments was to see if it was possible to get two separate phases, one pure iron phase, and one neodymium oxide phase. As seen from the results in section 4.3, the discussion above and the picture in Figure 28, this was not the case. Two phases that could be easily separated was not obtained. It still might be possible at higher temperatures and other oxygen partial pressures.

6 Conclusions

The magnetic waste was separated into four piles, and three of these were subsequently characterized by XRF. The weak magnets are probably ferrite magnets, based on the results from the analysis. The magnetic powder contained mostly silicon-, iron-, magnesium-, calsium- and aluminum oxides, and only 0.3111% rare earth elements. The strong magnets are believed to be Nd-Fe-B magnets based on appearance, strength and the XRF analysis.

The total rare earth content was calculated to be less than 5.5% which corresponds to 142g, and it is concluded that the recovery of rare earth elements from the magnetic waste is not profitable with today's technology.

Other methods for characterization should be examined, to get more reliable numbers for more elements. Several samples should also be characterized to get more statistically reliable results.

Neodymium was extracted from Nd-Fe-B magnets using molten silver, with different success rate. The extraction seems to increase with temperature, heating time and Ag:Nd ratio.

Analysis of the samples by EDS in SEM turned out not to be fully satisfactory, since it was hard to get unequivocal results.

Extraction of neodymium from Nd-Fe-B magnets by oxidation was attempted, but failed.

7   Future Work

In the future more more samples of magnetic waste should be examined to get statistically representative numbers. Other method should also be attempted, to get accurate numbers for more elements.

The mass flow of rare earth elements should be examined. It is important to get a good overview of how much rare earth elements that are present in electric and electronic equipment, and how much that is imported and recycled annually.

The method for extraction of neodymium from Nd-Fe-B magnets using molten silver should be examined more thoroughly, and new methods for separation of the Ag-Nd alloy and the Fe phase should be developed.

Extraction of neodymium from Nd-Fe-B magnets by oxidation should be examined at higher temperatures and other oxygen partial pressures.

Finally, other methods for element analysis of the samples should be considered.

8 References

Bristøl (2011)	Bristøl, L.M.L., Reduction and Recycling of Rare Earth Elements, TMT4500 Materials Technology, Specialization project, NTNU, Trondheim, Fall 2011
CRC (2011)	CRC, Handbook of Chemistry and Physics Online, 92nd edt, 2011
Ellis et al. (1994)	Ellis, T.W., Schmidt, F.A., Jones, L.L., Methods and opportunities in the recycling of rare earth based materials, Metallurgy and ceramics division, Ames laboratory, 1994
EPOW (2011)	European pathway to zero waste, Study into the feasibility of protecting and recovering critical raw materials through infrastructure development in the south east of England; Annexes , March 2011
EPOW (2011a)	European pathway to zero waste, Study into the feasibility of protecting and recovering critical raw materials through infrastructure development in the south east of England; Final report, March 2011
Gupta & Krishnamurthy (2005)	Gupta, C.K, Krishnamurthy, N., Extractive Metallurgy of Rare Earths, CRC Press, Boca Raton FL, USA, 2005
Itoh et al. (2004)	Itoh, M., Masuda, M., Suzuki, S., Machida, K., Recycling of rare earth sintered magnets as isotropic bonded magnets by melt-spinning, *J. Alloys and Compounds*, 374: 393-396, 2004
Motzfeldt (2004)	Motzfeldt, K., TMT4166 Experimental Materials Chemistry and Electro Chemistry, Ch. 2: Basic design of laboratory furnaces, p. 16, 2004
Öko-Institut (2011)	Öko-Institut e.V., Study on Rare Earths and Their Recycling, Darmstadt, January 2011
Öko-Institut (2012)	Öko-Institut e.V., Recycling critical raw materials from waste electronic equipment, Darmstadt, February 2012

Oakdene Hollins (2010)   Oakdene Hollins research & consulting, Lanthanide Resources and Alternatives, May 2010

Raghavan (2006)   Raghavan, V., Ag-Fe-Nd (Silver-Iron-Neodymium), *Journal of Phase Equilibria and Diffusion*, 27: 280, 2006

Saito et al. (2003)   Saito, T., Sato, H., Ozawa, S., Yu, J., Motegi, T., The extraction of Nd from waste Nd–Fe–B alloys by the glass slag method, *J. Alloys and Compounds*, 353: 189-193, 2003

SI Chemical Data (2002)   Aylward, G., Findlay, T., Si Chemical Data, 5th edition, John Wiley and sons, Australia, 2002

SGTE (2004)   SGTE; http://www.crct.polymtl.ca/fact/phase_ diagram.php?file=Fe-Nd.jpg&dir=SGTE Downloaded 01.06.12 at 17:20

Stølen & Grande (2004)   Stølen, S., Grande, T., Chemical Thermodynamics of Materials, John Wiley & Sons, England, p. 118-120, 2004

Swartzendruber (1984)   Swartzendruber, L.J., The Ag-Fe (Silver-Iron) System, *Bulletin of phase diagrams*, 5: 560-564, 1984

Sørløkk (2012)   Sørløkk, T., Senior Engineer Department of Geology and Mineral Resources Engineering, NTNU, Trondheim, Norway, personal communication, 2012.

Takeda et al. (2004)   Takeda, O., Okabe, T.H., Umetsu, Y., Phase equilibrium of the system Ag-Fe-Nd and Nd extraction from magnet scraps using molten silver, *J. Alloys and Compounds*, 379:305-313, 2004

Wang et al. (2009)   Wang, S.L., Wang, C.P., Liu, X.J., Ishida, K., Thermodynamic assessments of the Ag-Gd and Ag-Nd systems, *J. Alloys and Compounds*, 476: 245–252, 2009

WEEE Recycling AS (2011)   John Sunde, WEEE Recycling AS, Øysand Næringspark, Melhus, Information brochure and personal communication, 2011

West (2010)   West, A.R., Basic solid state chemistry, John Wiley & Sons, England, 2010

Zumdahl (2005)   Zumdahl, S.S., Chemical Principles 5th
                             edition, Houghton Mifflin Company, USA,
                             p. 941, 2005

Appendices

Appendix 1: Extraction of Neodymium using Molten Silver

The weights of magnets and silver used in the experiments are given in Table 7 below.

Table 8: The weights of magnets and silver used

Experiment	m_{Ag} [g]	m_{Mag} [g]	a_{Ag} [%]	a_{Nd} [%]	a_{Fe} [%]
1	54.36	34.79	50.78	7.78	41.44
2	53.32	35.22	49.99	7.91	42.10
3	32.74	21.34	50.32	7.85	41.82
4	29.69	18.99	50.79	7.78	41.43
5	23.97	7.63	68.20	5.03	26.77

Representative results from EDS analysis from each sample are given for both phases in Table 8 and 9.

Table 9: Representative results from the grey phase

Sample	Nd [wt%]	Ag [wt%]	Fe [wt%]	Ni [wt%]
1	2.72 ± 0.09	97.28 ± 2.82	0	0
2	12.43 ± 0.32	87.57 ± 2.41	0	0
3	15.36 ± 0.34	84.64 ± 2.02	0	0
4	12.49 ± 0.32	87.51 ± 2.42	0	0
5	31.16 ± 0.66	67.11 ± 1.61	0	1.73 ± 0.06

Table 10: Representative results from the black phase

Sample	Nd [wt%]	Ag [wt%]	Fe [wt%]	Ni [wt%]
1	0.26 ± 0.03	14.33 ± 0.35	81.99 ± 1.62	3.43 ± 0.09
2	0	0	97.65 ± 2.38	2.35 ± 0.08
3	0	0.05 ± 0.03	99.44 ± 2.01	0.51 ± 0.04
4	0	0	96.02 ± 2.24	3.98 ± 0.12
5	0	0	98.11 ± 2.18	1.89 ± 0.07

Appendix 2: Extraction of Neodymium by Oxidation

The weights of iron and magnets used in the experiments, and the molar percent are given in Table 10.

Table 11: Weights of iron and magnets used in oxidation experiments

Experiment	m_{Fe} [g]	m_{Mag} [g]	$n_{Fe}[\%]$	$n_{Nd}[\%]$	$w_{Fe}[\%]$	$w_{Nd}[\%]$
1	15.44	17.49	92.82	7.18	83.35	16.65
2	31.86	35.73	92.86	7.14	83.44	16.56

Appendix 3: Results from XRF Analysis on Magnetic Powder

Table 12: Results from the XRF analysis on the magnetic powder

	Sample 1[%]	Sample 2[%]	Sample 3[%]	Sample 4[%]	Av. [%]
SiO_2	18.52	18.61	19.04	18.82	18.75
Fe_2O_3	18.12	18.25	16.40	18.22	17.75
MgO	13.64	13.09	13.01	13.09	13.21
CaO	10.43	10.25	10.49	10.41	10.40
Al_2O_3	5.96	5.73	5.72	5.78	5.80
ZnO	3.89	3.78	3.74	3.77	3.80
TiO_2	1.65	1.63	1.67	1.63	1.65
PbO	1.22	1.24	1.32	1.24	1.26
SO_3	1.13	1.13	1.17	1.11	1.14
BaO	1.06	1.07	1.12	1.03	1.07
K_2O	0.8988	0.8898	0.9212	0.8976	0.9019
Na_2O	0.8089	0.7807	0.7411	0.7677	0.7746
CuO	0.7551	0.7382	0.7349	0.7318	0.7400
Cl	0.6042	0.6180	0.6084	0.6086	0.6098
MnO	0.5364	0.5497	0.5133	0.5721	0.5429
SrO	0.4405	0.4361	0.4622	0.4359	0.4437
Cr_2O_3	0.3816	0.3587	0.3470	0.3707	0.3645
ZrO_2	0.3526	0.2424	0.2085	0.2459	0.2624
P_2O_5	0.3513	0.3476	0.3375	0.3395	0.3440
SnO_2	0.3508	0.3447	0.3676	0.3448	0.3520
MoO_3	0.3232	0.3188	0.3325	0.3175	0.3230
NiO	0.3188	0.3207	0.2959	0.3190	0.3136
Nd_2O_3	0.2593	0.2735	0.2566	0.2338	0.2558
Br	0.2235	0.2256	0.2331	0.2184	0.2252
Sb_2O_3	0.0547	0.0586	0.0551	0.0506	0.0548
Y_2O_3	0.0349	0.0307	0.0281	0.0283	0.0305
CdO	0.0315	0.0295	0.0268	0.0317	0.0299
La_2O_3	0.0274	0.0236	0	0.0302	0.0203
V_2O_5	0.0263	0.0202	0.0225	0.0250	0.0235
Ag	0.0247	0.0246	0.0256	0.0244	0.0248
CoO	0.0243	0.0374	0.0262	0.0387	0.0317
Bi_2O_3	0.0209	0.0201	0.0211	0.0210	0.0208
Ho_2O_3	0.0178	0	0	0	0.0045
Nb_2O_5	0.0047	0.0039	0.0039	0.0053	0.0045
SeO_2	0	0.0037	0	0	0.0009
SUM	82.49	81.48	80.25	81.76	81.49

Appendix 4: Raw Data from XRF Analysis of Magnets

The raw data for the analysis of the strong magnets are given in Table 12.

Table 13: The raw data for the analysis of the strong magnets

Element	Magnet 1 [%]	Magnet 2 [%]	Magnet 3[%]	Magnet 4 [%]
Al	0 ± 80	0 ± 80	0 ± 80	0 ± 80
Ba	0 ± 0.012	0 ± 0.017	0.012 ± 0.009	0 ± 0.011
Sb	0 ± 0.005	0 ± 0.007	0 ± 0.007	0 ± 0.005
Sn	0 ± 0.005	0.065 ± 0.005	0.069 ± 0.005	0 ± 0.005
In	0 ± 0.003	0 ± 0.005	0 ± 0.004	0 ± 0.003
Cd	0 ± 0.002	0 ± 0.004	0 ± 0.004	0 ± 0.002
Pd	0 ± 0.002	0 ± 0.003	0 ± 0.003	0 ± 0.002
Ag	0 ± 0.009	0.424 ± 0.01	0.449 ± 0.01	0 ± 0.009
Mo	0 ± 0.018	0 ± 0.086	0 ± 0.041	0 ± 0.01
Nb	0 ± 0.007	0 ± 0.01	0.142 ± 0.007	0 ± 0.026
Zr	0 ± 0.003	0 ± 0.005	0 ± 0.005	0 ± 0.005
Bi	0 ± 0.017	0 ± 0.026	0 ± 0.027	0 ± 0.008
Pb	0.406 ± 0.015	0.501 ± 0.023	0.642 ± 0.024	0 ± 0.009
Hg	0.043 ± 0.005	0.087 ± 0.005	0.123 ± 0.01	0 ± 0.022
Br	0 ± 0.002	0 ± 0.003	0 ± 0.003	0.003 ± 0.001
Se	0 ± 0.099	0 ± 0.148	0 ± 0.155	0 ± 0.027
Au	0 ± 0.03	0 ± 0.047	0 ± 0.046	3.92 ± 0.052
Pt	0 ± 0.379	0 ± 0.563	0 ± 0.589	1.348 ± 0.047
Ta	0 ± 0.461	0 ± 0.615	0 ± 0.614	0.121 ± 0.034
Hf	0.672 ± 0.033	0.916 ± 0.05	1.163 ± 0.052	0.36 ± 0.029
Ni	72.291 ± 0.381	88.307 ± 0.48	92.533 ± 0.46	0.133 ± 0.02
Co	0.733 ± 0.041	0.806 ± 0.033	0.194 ± 0.023	0.157 ± 0.059
Fe	25.661 ± 0.107	7.288 ± 0.083	3.834 ± 0.057	93.416 ± 0.098
Mn	0.07 ± 0.012	0.958 ± 0.025	0.474 ± 0.018	0.271 ± 0.023
Cr	0.005 ± 0.002	0.255 ± 0.004	0.087 ± 0.002	0.221 ± 0.003
V	0.008 ± 0.002	0.099 ± 0.003	0.054 ± 0.002	0.01 ± 0.002
Ti	0.005 ± 0.002	0.064 ± 0.004	0.03 ± 0.002	0.009 ± 0.003

The raw data for the analysis of the weak magnets are given in Table 13.

Table 14: The raw data for the analysis of the weak magnets

Element	Magnet 1 [%]	Magnet 2 [%]	Magnet 3 [%]	Magnet 4 [%]
Al	0 ± 80	0 ± 80	0 ± 80	0 ± 80
Ba	0.248 ± 0.006	0.759 ± 0.013	0.197 ± 0.016	1.355 ± 0.009
Sb	0.014 ± 0.002	0 ± 0.006	0 ± 0.011	0.015 ± 0.002
Sn	0.015 ± 0.002	0 ± 0.007	0 ± 012	0.019 ± 0.003
In	0.042 ± 0.002	0 ± 0.004	0 ± 0.007	0.044 ± 0.002
Cd	0.064 ± 0.002	0 ± 0.003	0 ± 0.005	0.068 ± 0.002
Pd	0.089 ± 0.002	0 ± 0.002	0 ± 0.004	0.091 ± 0.002
Ag	0.089 ± 0.004	0.018 ± 0.007	0 ± 0.022	0.095 ± 0.005
Mo	0 ± 0.005	0 ± 0.013	0 ± 0.021	0 ± 0.005
Nb	0 ± 0.005	0 ± 0.01	0 ± 0.016	0 ± 0.005
Zr	2.253 ± 0.01	2.123 ± 0.018	2.292 ± 0.032	2.108 ± 0.01
Bi	0.02 ± 0.003	0.061 ± 0.006	0.056 ± 0.01	0.024 ± 0.003
Pb	0.119 ± 0.005	0.037 ± 0.008	0 ± 0.025	0.083 ± 0.005
Hg	0.009 ± 0.004	0 ± 0.014	0 ± 0.026	0 ± 0.008
Br	0.003 ± 0.001	0.006 ± 0.002	0.007 ± 0.003	0.003 ± 0.001
Se	0.024 ± 0.004	0.026 ± 0.008	0 ± 0.025	0.017 ± 0.004
Au	0.079 ± 0.007	0.074 ± 0.014	0 ± 0.044	0.069 ± 0.007
Pt	0 ± 0.03	0 ± 0.057	0 ± 0.091	0 ± 0.031
Ta	0.241 ± 0.019	0.164 ± 0.036	0 ± 0.115	0.205 ± 0.019
Hf	0.026 ± 0.01	0.05 ± 0.02	0 ± 0.057	0.021 ± 0.01
Ni	0.292 ± 0.016	0.288 ± 0.03	0.227 ± 0.05	0.292 ± 0.017
Co	0.272 ± 0.036	0 ± 0.132	0 ± 0.22	0.251 ± 0.037
Fe	95.688 ± 0.107	95.268 ± 0.093	96.712 ± 0.152	94.843 ± 0.051
Mn	0.41 ± 0.014	0.329 ± 0.026	0.246 ± 0.041	0.387 ± 0.015
Cr	0 ± 0.002	0.085 ± 0.003	0 ± 0.002	0 ± 0.002
V	0 ± 0.002	0.182 ± 0.005	0 ± 0.002	0 ± 0.002
Ti	0 ± 0.002	0.431 ± 0.008	0 ± 0.002	0 ± 0.002